28.8 A MOS Image Sensor with Microlenses Built by Sub-Wavelength Patterning

Kimiaki Toshikiyo, Takanori Yogo, Motonori Ishii, Kazuhiko Yamanaka, Toshinobu Matsuno, Kazutoshi Onozawa, Takumi Yamaguchi

Matsushita Electric Industrial, Kyoto, Japan

In addition to scaling down the pixel size of the imaging devices for digital still cameras and cell phone cameras [1-3], miniaturization of the camera modules themselves has become a major concern in recent years. Shortening the distance between the objective lens and the image sensor is critical to achieving this goal. However, when this distance is reduced, the efficiency of the light-collection is significantly reduced at the image sensor periphery due to the highly increased incident angle of the incoming light as shown in Fig. 28.8.1. Therefore, to provide uniform light-collection efficiency over the imaging surface is extremely important. To overcome this problem, we have developed a MOS image sensor with a new type of on-chip lenses, digital-microlenses (DMLs). DMLs enable us to use optimized offset focusing adapted to the pixel position and for different RGB wavelengths. The present DML is implemented by the sub-wavelength patterning of concentric SiO_2 ring walls. The refractive index profiles are optimized from pixel to pixel depending on the location of the pixel. As a result, a 1/3.2 inch, 3Mpixel MOS image sensor based on the DML technology exhibited excellent uniformity of light-collection efficiency across the image sensor area even for light with a very large incident angle of over 45°, which has never been attained by conventional thermally-deformed polymer microlenses.

Figure 28.8.2 illustrates the design principle of DMLs with distributed refractive indices. In order to realize the typical arcs of conventional microlenses, the large modulation of refractive index, n_1, plotted in the top row on the left side is necessary. In this example n_1 is greater than 3. Such a profile is impossible with transmissive materials commonly used in semiconductor processes. Therefore, by using Fresnel diffractive theory [4], we convert $n_1(r)$ into the Fresnel-type profile of refractive index $n_2(r)$, as plotted in the middle row. The resulting desired refractive index profile is attained by using low refractive index materials, in which the maximum of $n_2(r)$, n_2, is less than 2. The desired profile can be duplicated by a DML made up of multiple rings with different widths and radiuses. These rings are made out of SiO_2 and the separation between two adjacent rings is set to be less than the wavelength of the incoming visible light. The region between the walls is an air gap. It is noted that the resulting refractive index profile is equivalent to an arc of a microlens centered on the pixel. This is the configuration in which the light-collection efficiency is optimized for a 0° incident angle of the incoming light. In order to realize the required high light-collection efficiency for the pixels on the periphery of the image sensor, an off-centered refractive index profile is required, as plotted at the top right-hand side of the figure. This pattern is achieved by displacing the center of the rings from the center of the pixel as shown in the bottom figure. As a result, it is equivalent to forming an off-center arc microlens on the pixel. Thus, the main problem reduces to defining a refractive index profile for each DML as a function of the incident angle of incoming light, θ.

The targeted refractive index profile is derived from four components: (1) a component proportional to the square of position (r^2), which realizes the function of light collection; (2) a term that varies with the product of the position (r) and the incident angle (θ), which leads to the displacement of the optical axis of the DML; (3) a term containing $\sin^2\theta$ to compensate for the displacement of the optical axis; and (4), a phase factor with the period of 2π. Summing up these components, the desired refractive index profile $n(r)$ is parametrically expressed as

$$n(r) = n_0 + \frac{\Delta n_{max}}{2\pi}\left(-\frac{K_0 n_1}{2f}r^2 - K_0 n_0 r \sin\theta - \frac{K_0 n_0^2 f \sin^2\theta}{2n_1} + 2\pi D\right), \qquad (1)$$

where D is natural number, n_0 and n_1 are the refractive indices on the side from which the light enters the lens (air) and the side from which the light exits the lens (SiO_2), respectively, Δn_{max} is the difference in n_0 and n_1, K_0 is the magnitude of the wave number ($2\pi/\lambda$), f is the focal length of DML and λ is the wavelength of the light.

Figure 28.8.3 shows a mapping of the output signals from 8×10 unit areas, each of which consists of 180×160 pixels with identical DMLs having the same designed offset angle (θ). As θ increases in the horizontal direction, the center of the concentric SiO_2 rings is displaced from the center of the pixel. The incident angle (α) of the incoming light is also varied and the output signals are plotted in the vertical direction. As designed, the output signal is maximized (most whitish) when the incident angle is equal to the designed offset angle. This proves that the light-collection efficiency is optimized for different incident angles by manipulating the ring configuration of the DML.

In Fig. 28.8.4, a chip micrograph of a MOS image sensor integrated with DMLs is shown. The pixels are arranged in a 2064×1553 (or 3Mpixel) array in a 1/3.2 inch optical format. The size of each pixel is 2.2×2.2μm². As shown in the inset SEM micrographs, the DMLs are centered on the pixel center for the pixels located in the central region. The DMLs with their optical axes displaced from the pixel centers are used for the pixels on the periphery. The minimum width of the SiO_2 ring wall is 0.1μm and the maximum aspect ratio of the ring wall is 8. The circuit shown on the right side of Fig. 28.8.4 contains only four major elements: a floating diffusion (FD), a reset transistor, a detect transistor, and a transfer transistor. The first two transistors are shared by four pixels resulting in a total of only 1.5 transistors per pixel. A small size pixel is realized by reducing the number of transistors per pixel. Then, the manipulation of the on-chip optical elements is critical. From the consideration of the minimum unit of the controllable ring volume ratio, the DML technology is applicable to MOS image sensors with pixel sizes smaller than 1.0×1.0μm², which is not achieved by conventional polymer microlenses.

The measured light-collection efficiency of the image sensor as a function of incident angle is shown in Fig. 28.8.5. The light-collection efficiency is normalized at the incident angle of 0°. As explained in Fig. 28.8.1, the incident angle of the incoming light is 0° for the pixels in the central region while the angle is highest at the edge of the image sensor. Thus, the position of the pixels can be converted to the incident angle which is represented by the horizontal axis of the figure. The light-collection efficiency of the image sensor with conventional microlenses drops sharply when the incident angles are larger than 30° and is down to 30% for the pixels near the edge. In contrast, the DML integrated MOS image sensor achieves a light-collection efficiency of 60% even for incident angles over 45°. As a result, the DML integrated image sensor exhibits extremely uniform brightness across the plane of the reproduced image, while the conventional image sensor suffers from reduced brightness on the periphery due to the low light-collection efficiency. Finally, the chip performance of the present DML integrated MOS image sensor is summarized in Fig. 28.8.6.

Acknowledgements:
The authors are grateful to Dr. Yutaka Hirose, Dr. Yasuhiro Shimada and Dr. Daisuke Ueda for their continuous encouragement.

References:
[1] M. Mori et al., "A 1/4in 2M Pixel CMOS Image Sensor with 1.75Transistor/Pixel," *ISSCC Dig. Tech. Papers*, pp. 80-81, Feb., 2004.
[2] M. Kasano et al., "A 2.0μm Pixel Pitch MOS Image Sensor with an Amorphous Si Film Color Filter," *ISSCC Dig. Tech. Papers*, pp. 348-349, Feb., 2005.
[3] M. Oda et al., "A 1/4.5in 3.1M Pixel FT-CCD with 1.56μm Pixel Size for Mobile Applications," *ISSCC Dig. Tech. Papers*, pp. 346-347, Feb., 2005.
[4] D. O'Shea et al., ed., Diffractive Optics Design, Fabrication, and Test, SPIE PRESS, 2004.

 1-4244-0852-0/07/$25.00

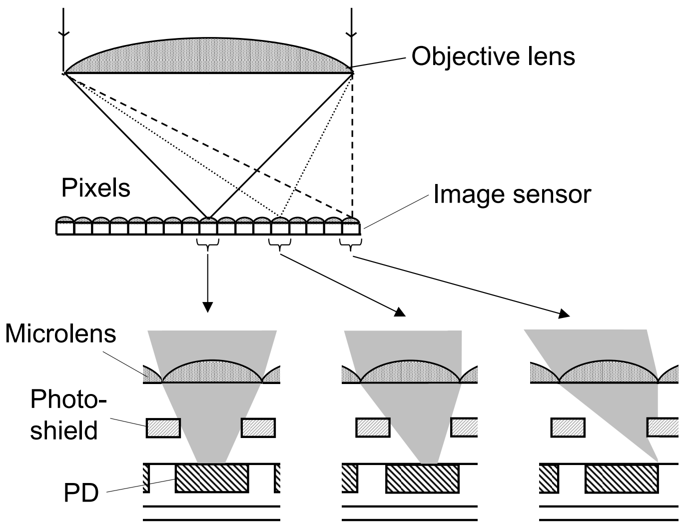

Figure 28.8.1: Schematic illustrations of a camera module with ultra-short focal length.

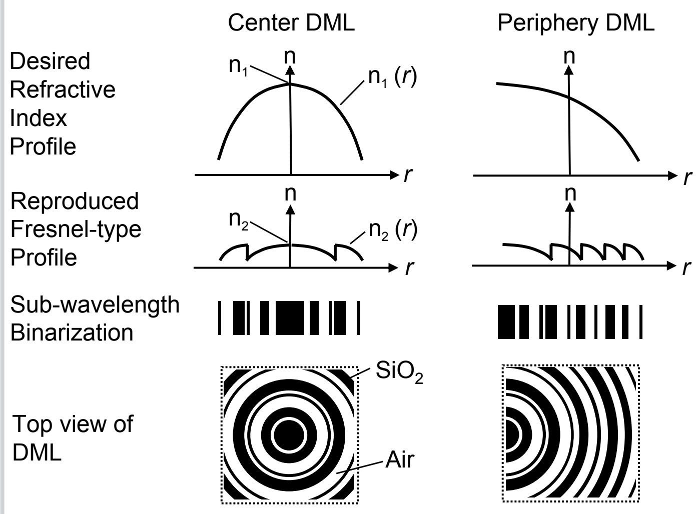

Figure 28.8.2: The design principle for DMLs.

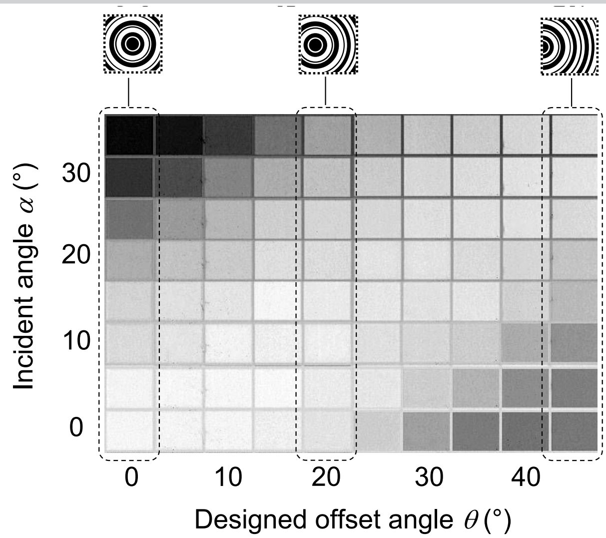

Figure 28.8.3: A brightness map of white light images corresponding to collection-efficiency mapping as functions of designed offset angle (θ) and of incident angle (α).

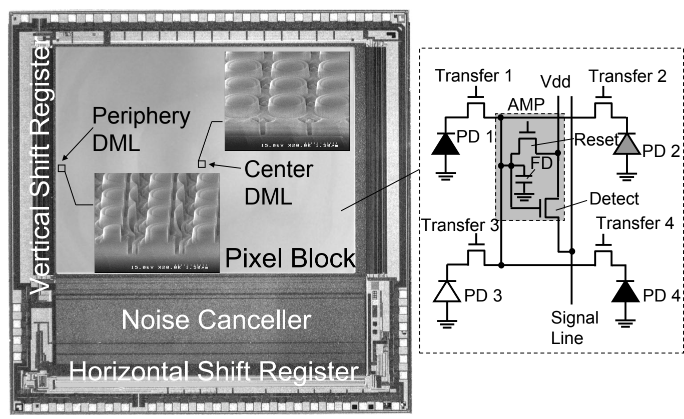

Figure 28.8.4: Chip micrograph showing the chip architecture (left) and circuit configurations (right).

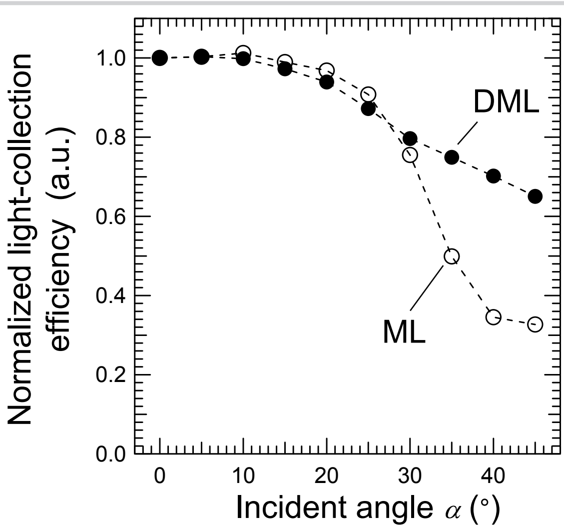

Figure 28.8.5: Normalized light-collection efficiencies as functions of incident angle α for a DML integrated image sensor and for a conventional image sensor (ML).

Pixel size	2.2 μm × 2.2 μm
Optical format	1/3.2 inch
The number of pixels	2064 (H) x 1553 (V) = 3 M
Technology	0.15μmCMOS(1P, 2M)
Number of transistors per pixel	1.5
Lens	Digital microlens
Lifetime	> 200,000 hours
Heat resistance	> 300 °C

	DML	Conventional lens
Sensitivity (Center)	4200 electrons/lx·s	4100 electrons/lx·s
Sensitivity (Periphery)	3000 electrons/lx·s	1300 electrons/lx·s

Figure 28.8.6: Summary of the chip performance.

28